Institute of Physics Publishing Smart Materials and Structures

Smart Mater. Struct. **14** (2005) 561–568 doi:10.1088/0964-1726/14/4/014

Passive wireless strain monitoring of tyres using capacitance and tuning frequency changes

Ryosuke Matsuzaki[1,3] **and Akira Todoroki**[2]

[1] Tokyo Institute of Technology, Japan, 2-12-1, Ohokayama Meguro, Tokyo 1528552, Japan
[2] Department of Mechanical Sciences and Engineering, Tokyo Institute of Technology, Japan, 2-12-1, Ohokayama Meguro, Tokyo 1528552, Japan

E-mail: rmatsuza@ginza.mes.titech.ac.jp

Received 28 April 2004, in final form 1 December 2004
Published 4 May 2005
Online at stacks.iop.org/SMS/14/561

Abstract
In-service strain monitoring of tyres of automobiles is quite effective for improving the reliability of tyres and anti-lock braking systems (ABS). Conventional strain gauges have high stiffness and require lead wires. Therefore, they are cumbersome for tyre strain measurements. In a previous study, the authors proposed a new wireless strain monitoring method that adopts the tyre itself as a sensor, with an oscillating circuit. This method is very simple and useful, but it requires a battery to activate the oscillating circuit. In the present study, the previous method for wireless tyre monitoring is improved to produce a passive wireless sensor. A specimen made from a commercially available tyre is connected to a tuning circuit comprising an inductance and a capacitance as a condenser. The capacitance change of the tyre alters the tuning frequency. This change of the tuned radio wave facilitates wireless measurement of the applied strain of the specimen without any power supply. This passive wireless method is applied to a specimen and the static applied strain is measured. Experiments demonstrate that the method is effective for passive wireless strain monitoring of tyres.

(Some figures in this article are in colour only in the electronic version)

1. Introduction

Recently, to improve the safety of automobiles, smart tyres equipped with sensors for monitoring strain, air pressure and the temperature of the tyres have been under development [1–13]. As a result of the recall of Firestone Co. tyres, US transportation recall enhancement, accountability, and documentation (TREAD) legislation has mandated installation of tyre pressure monitoring systems (TPMSs) [1–5]. A tyre strain monitoring system with sensors that transmit the tyre strain signal to an anti-lock braking system (ABS) or electronic stabilization program (ESP) system is demanded to enhance tyre reliability and produce TPMS at lower cost.

ABS enables one to improve the control of the force of the braking system and minimize the distance for stopping using information on the friction between the tyres and the road surface. Current ABS installations, however, do not measure the friction directly. Instead, they calculate it indirectly by monitoring the rotation speed of each individual tyre at the respective axle, which engenders a time lag and measurement error. Direct monitoring of tyre strain allows precise measurement of friction, and hence it increases the efficiency of ABS [6]. Smart tyres also have beneficial effects on other advanced active safety systems such as traction control systems (TCSs) and vehicle stability assist (VSA), early tyre-separation detection [7] and tyre-burst prevention [8].

Several required specifications exist for tyre sensors for installing smart tyres. First, wireless monitoring is indispensable because a tyre usually rotates. Therefore, it is difficult to use wired sensors. Second, because tyre rubber typically has low stiffness, embedding or attaching the sensors easily disturbs the tyre stress or deformation: sensors should

[3] Author to whom any correspondence should be addressed.

not cause such a disturbance. Third, the large difference of stiffness of the sensors from that of rubber may cause debonding between the sensors and the rubber over a long running time: the stiffness difference should be small. Fourth, the sensor must be inexpensive because the tyre itself is not an expensive product compared to aerospace components or building structures in which an expensive sensor can be used.

Most sensors employed for the smart tyres sacrifice one or two of these required specifications. For example, surface acoustic wave (SAW) sensors [6] are usually generated using piezoelectric ceramics. Such sensors require a special tool, like a pin, to reduce tyre deformation and enhance force because of the deformation. This implies that SAW sensor implementation causes a disturbance attributable to tyre deformation or stress.

Microelectromechanical systems (MEMSs) for wireless strain measurement are embedded in smart composite structures [14, 15]. Wireless MEMSs include a sensor, a signal processing unit, and an antenna. The wireless MEMS strain sensor is an attractive device, but embedding the MEMS sensor into a tyre is not recommended because of the large difference in stiffness between the sensor and the rubber tyre. This large difference in stiffness may disturb the deformation and stress; it may also cause debonding of the sensors and rubber over a long period of use.

Conventional strain gauges present a similar problem to that of wireless MEMSs. A small wireless data transfer chip can be applied to conventional strain gauges to transfer data wirelessly. However, even for the strain gauge, the large difference in stiffness and weak bonding between the strain gauge and the rubber may cause debonding during a long period of service. High-cost sensor systems such as optical fibre systems [9] are not feasible because tyres themselves are not expensive products. Therefore, a novel sensor is demanded for a true ‘smart tyre’.

Tyres comprise rubber with carbon black, steel wire, and organic fibre. Steel wire belts are inserted under the tread rubber. The steel wire itself is an electrically conductive material and the rubber is a dielectric material. This tyre structure is quite similar to that of an electrical condenser, which comprises a pair of electrodes and an intervening dielectric material: tyre deformation changes spacing between the steel wires, which consequently changes the capacitance of the tyre part. Measurement of that tyre capacitance change indicates the tyre strain or deformation without the need for embedding or attaching additional sensors.

In a previous study [10], the authors proposed a new wireless strain monitoring method that adopts the tyre itself as a sensor, with an oscillating circuit. In that method, steel wires are employed as electrodes to measure tyre capacitance changes. A specimen cut from a commercial tyre is connected to an oscillating circuit. The oscillation frequency changes with the capacitance changes of the tyre. This method is extremely simple and useful, but it requires a battery to activate the oscillating circuit.

The present study improves the previous method for wireless tyre monitoring to produce a passive wireless sensor. A specimen made from a commercially available tyre is connected to a tuning circuit comprising an inductance and a capacitance as a condenser. The change in capacitance of the tyre alters the tuning frequency. This frequency change allows wireless measurement of the applied strain of the specimen using no external power supply. This novel passive wireless method is applied to a specimen and the static applied strain is measured.

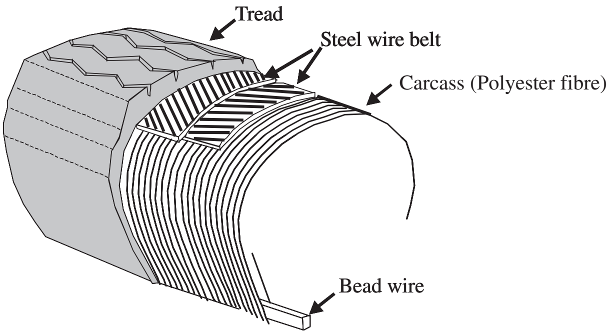

Figure 1. Inner structure of a steel-wire-reinforced radial tyre.

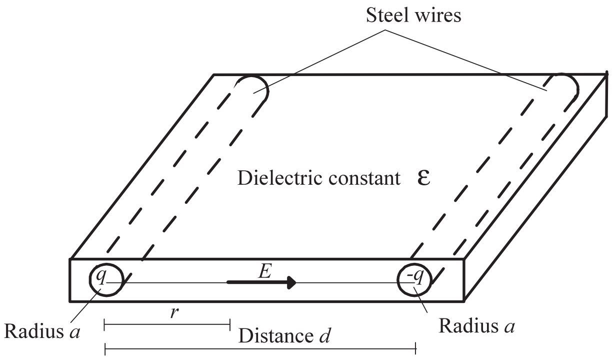

Figure 2. Condenser model of a steel wire belt of a tyre.

2. Wireless strain monitoring system

This passive wireless strain measurement system employs the tyre itself as a sensor. Figure 1 shows the inner structure of a typical radial tyre. The carcass fibres are perpendicular to the beads wire on radial tires as shown in figure 1. The carcass is the main element of the tyre, including the section inside the tread, the sidewall, and the bead section. The carcass’s function is to maintain the shape of the tyre. This carcass is composed of two layers of rubber-coated cord called carcass fibre. Usually, the carcass fibre is made from organic fibres such as polyester. Steel wire layers are mounted on the carcass fibre layer in a similar manner to cross-ply laminates of composite materials. These rubber-coated fibres and the tread rubber layer are mounted on the steel wire layers, as shown in figure 1. Tread deformation is transferred to the steel wire layers. When the tyre tread deforms with the rotation of the tyre, the deformation of the tread is transferred to the steel wire layers. Thereby, measurement of the strain of the steel wire layer enables us to know the tyre tread deformation.

In the steel wire layer, the steel wire is a straight electrical conductive material and the rubber is a dielectric material. Two adjacent steel wires are placed face to face and dielectric rubber is inserted between the two steel wires, as shown in figure 2.

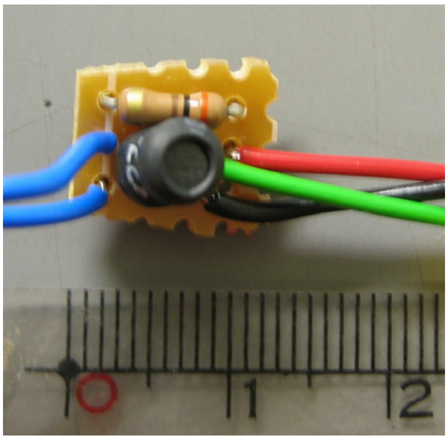

Figure 3. Appearance of the tuning circuit.

Electric voltage is charged between the steel wires. Therefore, this structure resembles an electrical condenser. The adjacent steel wires are electrodes of an electric condenser.

When the adjacent steel wires are given electrical charges per unit length, q, $-q$, respectively, from Gauss's law, the electrical field on the line through centres of the adjacent steel wires, E, at the distance, r, from a steel wire shown in figure 2 is given as

$$E = \frac{q}{2\pi\varepsilon r} + \frac{q}{2\pi\varepsilon(d-r)}, \tag{1}$$

where ε is the dielectric constant of the rubber and d is the space separating the adjacent steel wires.

Equation (1) shows the difference in potential between adjacent steel wires, V, as

$$V = -\int_{d-a}^{a} E_r \,\mathrm{d}r = \frac{q}{\pi\varepsilon} \ln\left(\frac{d-a}{a}\right), \tag{2}$$

where a is the radius of the steel wire within the tyre.

Equation (2) implies that the condenser's capacitance per unit length, C, is

$$C = \frac{q}{V} = \frac{\pi\varepsilon}{\ln\frac{d-a}{a}}. \tag{3}$$

For a large number of steel wires inside the tyre, the capacitance is calculated from kC using a number of modelled condensers, k. Spacing d is enlarged when the steel wire layer is elongated, indicating by virtue of equation (3) that the capacitance is reduced. Capacitance increases when the steel wire layer shrinks. Tyre deformation alters the capacitance of the tyre.

The present study adopts a simplified passive tuning circuit as shown in figure 3 for sending the capacitance change of the tyre to a receiver wirelessly. Figure 4 shows a schematic image of the present passive wireless monitoring system. The systems comprise an external transmitter, a strain sensor, and an external receiver. The wireless strain measurement system uses four antennas, including one for the output of the external transmitter, two for the input and the output of the sensor module, and one for the input of the external receiver. The antennas used are wire type and 150 mm long.

The transmitter is employed here to emit radio waves of white noise. It is easily produced using a normal function generator. The transmitted white noise is picked up with the tuning circuit antenna. The tuning circuit comprises the inductance (L in henries) of a coil, the capacitance (C_x in farads) of a tyre specimen, and a resistance. This is a pure L–C parallel resonator circuit. The impedance of the resonant circuit, Z, is given as

$$Z = \frac{1}{\mathrm{j}(\omega c_x - \frac{1}{\omega L})}, \tag{4}$$

where j is $\sqrt{-1}$, and ω is the radian frequency in hertz.

The denominator of equation (4) is set equal to zero to find the strain sensor tuning frequency, f_t:

$$\omega C_x - \frac{1}{\omega L} = 0. \tag{5}$$

Solving equation (5), the tuning frequency is given as

$$f_\mathrm{t} = \frac{\omega}{2\pi} = \frac{1}{2\pi\sqrt{LC_x}}. \tag{6}$$

Rearranging equation (6), the capacitance C_x can be determined as follows:

$$C_x = \frac{1}{L(2\pi f_\mathrm{t})^2}. \tag{7}$$

This equation shows that the increase in capacitance C_x decreases the tuning frequency when the inductance L is fixed. When the applied stress deforms the tyre specimen, the tyre specimen capacitance changes. Consequently, deviation occurs from the tuning circuit resonance. The tuned radio wave at frequency f_t is picked up at the external receiver. Its frequency is calculated by means of fast Fourier transformation (FFT). Equation (7) shows that measurement of the frequency change indicates the change of the tyre's capacitance, which indicates the tyre deformation. Since the antenna at the external receiver can receive the signal from the sensor as well as the direct signal from the transmitter, an electromagnetic shield is needed between the white noise area and the sensor output area. The white noise area includes the output antenna of the external transmitter and the input antenna of the sensor module. The sensor output area includes the output antenna of the sensor module and the input antenna of the external receiver. In a practical use, the output antenna of the external transmitter and the input antenna of the sensor are placed inside of the tyre, and the output antenna of the sensor and the input antenna of the external receiver are placed outside of the tyre, such as on a tyre wheel.

This monitoring system provides three main advantages. First, the tyre itself is adopted as a sensor. Thereby, this method avoids sensor debonding during a long period of service and disturbance of the tyre stress and deformation field. Second, the strain sensor system is of passive wireless type. Such a passive wireless sensor requires no batteries to activate the sensor circuit. This method achieves weight reduction and long-term stabilization. Third, electromagnetic waves are used for wireless passive communication. A sensor using electromagnetic induction [11] for wireless passive communication is apt to be affected by the radio range and the radio range is very short. Since the sensor proposed here uses electromagnetic waves instead of electromagnetic induction, the sensor does not have those problems.

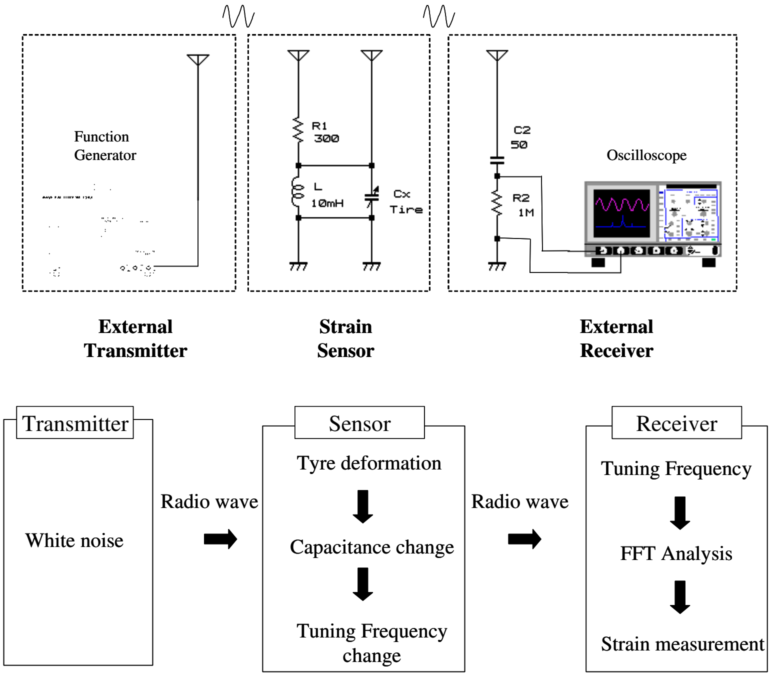

Figure 4. Schematic image of the wireless strain measurement system.

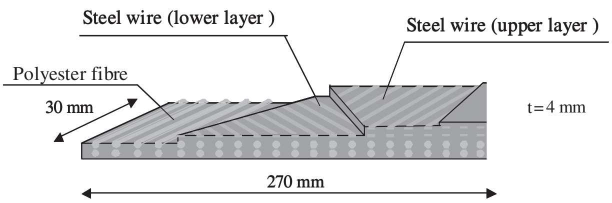

Figure 5. Tyre specimen configuration.

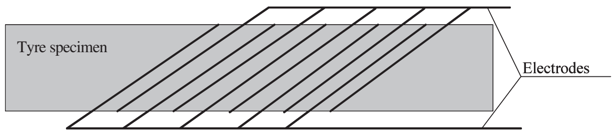

Figure 6. Interdigital electrodes ($N_d = 10$).

3. Experimental procedure

3.1. Specimens

The specimen employed in the present study is taken from a commercially available radial tyre. The proposed system can be applied as an attached or embeddable patch, like a strain gauge, instead of using actual steel wires of a radial tyre. The patch-type system is similar to a conventional strain gauge. Using actual steel wires of tyre can be more effective for measuring tyre deformation. However, it requires further trials, which will be undertaken in future studies.

Figure 5 shows the specimen configuration. The specimen length, width, and thickness are 270, 30, and 4 mm, respectively. The longitudinal direction of the specimen is the circumferential direction of tyre. In this specimen, 1.0 mm diameter steel wires are embedded in parallel with 2.5 mm spacing. The fibre angle is about $\pm 20°$ to the longitudinal direction of the specimen. The steel wire surface is covered with a special surface treatment to improve the bonding between the steel and rubber. That surface treatment is removed from the wire with a sheet of sandpaper. After polishing, two lead wires are soldered to the steel wires to produce two electrodes. A conventional strain gauge that is designed for rubber is attached to the specimen surface between the two electrodes to measure the applied strain.

An interdigital electrode, similar to that shown in figure 6, has been investigated for enhancing the tyre capacitance change attributable to applied strain in the previous study [11]. Steel wires in the tyre specimen are used as interdigital electrodes. The number of electrodes used, N_d, is 10. Increasing N_d implies increasing the number of capacitors in the tyre specimen, thereby increasing the capacitance change. The value of N_d is set to a maximum limit at 10 in this study to prevent increase of the sensing area.

3.2. Measurement of change in capacitance

Static tension tests are performed initially to measure the capacitance change of the specimen during loading and unloading. Figure 7 shows the experimental set-up composed of a static material testing machine produced by Shimadzu Corp., an LCR meter (No 3522; Hioki E. E. Corp.) produced by a tyre specimen, and a computer. For measurement, the charged alternating current is 100 kHz because the tuning frequency mentioned later is about 100 kHz. The applied strain is also measured with a conventional strain gauge attached to the specimen surface. Tensile tests are performed at a stroke speed of 1.0 mm min^{-1} and up to 3 mm of displacement. Subsequently, unloading is performed. Capacitance is measured without stopping the loading. A silicone rubber sheet is inserted between the jig and the specimen to prevent electrical shorts that might occur between the specimen and the testing machine jigs.

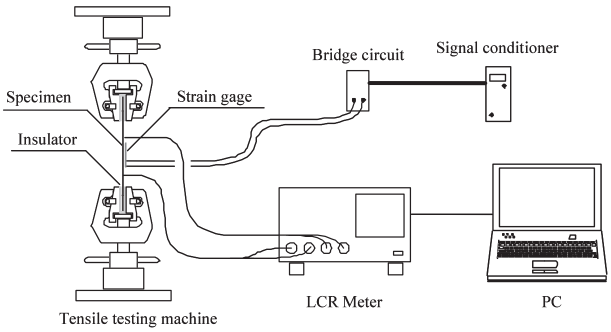

Figure 7. Experimental set-up for capacitance measurement.

3.3. Static tension test

Static tension tests using the sensor are performed to check the feasibility of the wireless passive monitoring system. A micro-inductor of 10 mH is used as the constant inductor of the tuning circuit, L. A tyre specimen with interdigital electrodes ($N_{\rm d} = 10$) is used as the capacitance C_x. A static tensile test is performed at stroke speed of 1.0 mm min^{-1} and up to 3 mm of displacement. Unloading is performed after that. Tuning frequency change attributable to the change of the applied tensile strain of the tyre is measured during loading and unloading using a digital oscilloscope. A silicone rubber sheet is inserted between the jig and the specimen.

3.4. Cyclic loading test

Since the tuning frequency of the sensor output changes dynamically with the tyre deformation, time–frequency analysis is needed to analyse this non-stationary tuning frequency. Time–frequency analysis of a non-stationary signal provides a simultaneous time and frequency domain representation of the signal. However, the FFT, which is the most common method for frequency analysis, assumes a stationary analysis target. A frequency function is produced when FFT is performed on a non-stationary signal. It has no information regarding the time.

Short-time Fourier transformation (STFT) has been developed as a solution for time–frequency analysis. The STFT is based on the assumption that signals are stationary over a short time. The STFT divides the signal into small time segments using a window function and performs Fourier transforms on each segment of the time to derive the spectrum. The power density spectrum, $S(t, \omega)$, of a signal $s(t)$ obtained through STFT is expressed as

$$S(t, \omega) = \int s(\tau) h(\tau - t, \Delta t) \mathrm{e}^{-\mathrm{j}\omega\tau}\, \mathrm{d}\tau, \qquad (8)$$

where $h(t, n)$ is a window function centred at time t and Δt is the length of the small time segment. The energy density spectrum of the STFT is defined as

$$P(t, \omega) = |S(t, \omega)|^2. \qquad (9)$$

The length of short-term stationarity determines the frequency resolution. An advantage of the STFT method is that it allows signals of long duration to be captured in small fragments with the assumption of a stationary representation for the short capture duration. The present study uses the window function $h(t, n)$ for a Hanning window, which detects a small power spectrum [16].

$$h(t, n) = \begin{cases} 0.5 - 0.5\cos\left(\dfrac{2\pi n}{N-1}\right) & (|t| \leqslant \Delta t/2) \\ 0 & (|t| > \Delta t/2). \end{cases} \qquad (10)$$

However, the STFT faces the indeterminacy principle: increased time resolution decreases the frequency resolution. In this respect, the maximum entropy method (MEM) is known to be a method offering better frequency resolution than FFT. The MEM is effective for frequency measurement at the spectrum peak because it applies a polynomial approximation to the spectrum peak. The MEM also offers the advantage of noise insensitivity. To analyse non-stationary signals, short-time MEM (STMEM) is performed by means of repeating the MEM on the assumption that signals are stationary on a short-time basis, as is the case with the STFT. Details of STFT and MEM are described in the references (for example, see [17, 18]).

Figure 8 shows the software window used to monitor the tuning frequency in real time. Table 1 shows software specifications. The method time–frequency analysis is optional: either STFT or STMEM can be used. The sampling frequency of the input signal is up to 500 Hz; the sampling frequency of the power spectrum is about 100 Hz. This specification allows measurement of the tuning frequency change up to 10 Hz.

Table 1. Specification of the software.

Sampling frequency of voltage	1–500 Hz
Frequency range	0–250 Hz
Spectrum analysis method	STFT, STMEM
Spectrum sampling frequency	−100 Hz

The cyclic loading test is performed to investigate the feasibility of monitoring change in the tuning frequency using STFT or STMEM. The specimen shown in figure 5 is loaded cyclically to measure the tuning frequency change wirelessly with the software. The stroke displacement is 3.0 mm, and the stroke frequencies are 0.5, 1, 5, and 10 Hz, which correspond to vehicle velocities of about 3, 6, 30, and 60 km h^{-1}, respectively. The strain gauge is easily damaged because of the different stiffness between the tyre surface and the strain gauge during cyclic loading tests; tyre strain is determined using the stroke displacement.

4. Results and discussion

4.1. Measurement of change in capacitance

Figure 9 shows the change in capacitance between interdigital electrodes ($N_{\rm d} = 10$) of the tyre specimen during loading and unloading cycles. The abscissa is the applied strain measured using the strain gauge; the ordinate is the measured capacitance change of the tyre specimen. This figure illustrates that the capacitance increases concomitantly with the increase of tensile loading from about 170 to 270 pF. Equation (3) shows that increased capacitance implies a decrease of spacing between the steel wires during tensile loading. Tensile loading

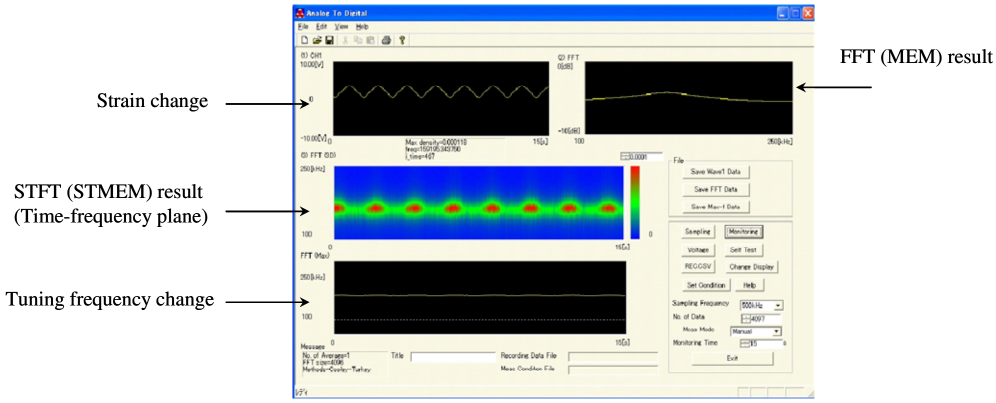

Figure 8. Developed software for spectrum monitoring.

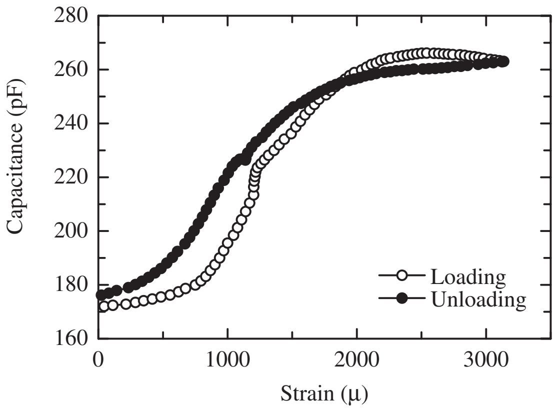

Figure 9. Measured capacitance change during loading and unloading.

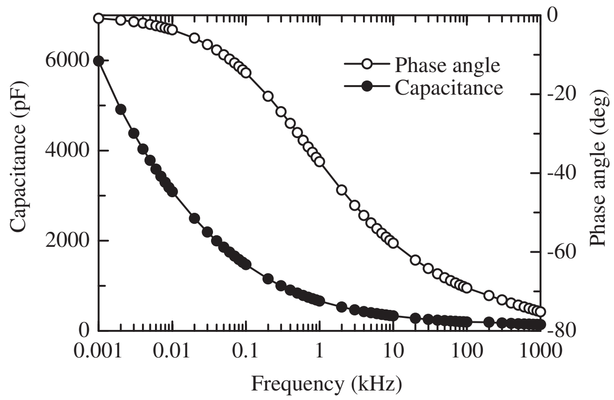

Figure 10. Frequency response of the capacitance and phase angle of the tyre specimen.

rotates the wire because the steel fibre angle is about 20°, measured by means of a protractor. That rotation decreases the wire angle; thereby, the transverse compressive strain decreases the specimen width. These phenomena decrease the spacing during tensile loading. Figure 9 shows that the change of capacitance has an upper limit in the strain region over 3000 $\mu\varepsilon$, and there is a small hysteresis loop of the measured capacitance during loading and unloading. For an actual tyre, the maximum deformation is approximately 2000 or 3000 $\mu\varepsilon$. Therefore, this limit is not a serious problem for actual measurement.

Figure 10 shows frequency response characteristics of the tyre specimen capacitance. The abscissa is the frequency of the charged alternating current; the ordinate is the measured capacitance and phase angle of the specimen impedance. This figure reveals that, with increased frequency, the phase angle decreases and approaches −90°. Therefore, the tyre specimen can be regarded as an electrical condenser in the high-frequency range. The capacitance from 10 to 1000 kHz is almost the same and its value is 200 pF as shown in figure 10. From the inductance L of 10 mH and the equation (6), the calculated tuning frequency is about 112 kHz.

4.2. Static tension test

Figure 11 shows the result for power spectra of the white noise, the sensor output, and a radio wave picked up with the receiver

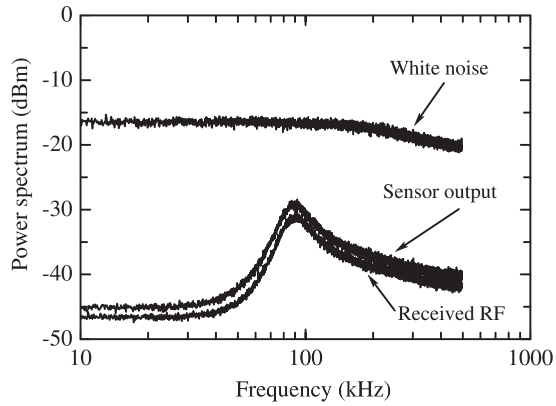

Figure 11. Measured power spectrum of white noise, sensor output, and received RF signal.

under a no-loading condition. In this figure, the abscissa is the frequency; the ordinate is the measured power spectrum. Although the power spectrum of white noise is constant for a frequency change, the power spectra of the sensor output and the received wave have peaks at the tuning frequency of 100 kHz. This means that only the tuned waves in the white noise are passed through the passive wireless sensor.

Figure 12 shows results of static tension tests of the specimen using the proposed passive wireless system. In this

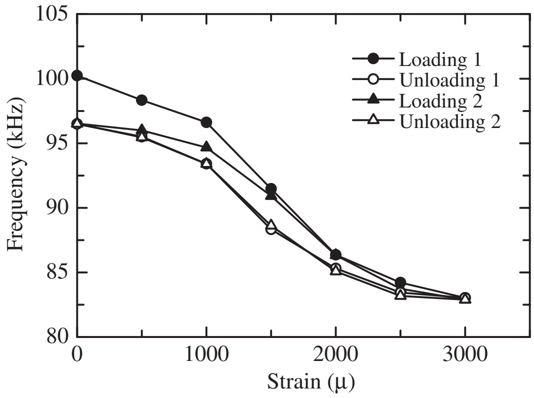

Figure 12. Measured relationship between strain and tuning frequency change of the passive wireless sensor.

figure, the abscissa is the applied strain measured using the attached strain gauge. The ordinate is the tuning frequency picked up with the receiver. The tuning frequency, f_t, is determined from the frequency at a maximum point of the power spectrum obtained with FFT. Static tension tests are performed twice: first loading (solid circle symbol), first unloading (open circle symbol), second loading (solid triangle symbol), and second unloading (open triangle symbol).

The measured resonant frequency, f_r, decreases with increased tensile strain, as shown in figure 12, corresponding to an increase of capacitance accompanying an increase in tensile strain, as shown in figure 8. Results obtained from figure 12 indicate that the proposed method is applicable for wireless strain measurement of commercially available tyres.

4.3. Cyclic loading test

Figures 13(a) and (b) show the measured frequency change attributable to the cyclic loading at stroke frequencies of 1 and 10 Hz, respectively, by means of the STMEM. Because measurement using STFT is sensitive to noise, it is difficult to distinguish the spectrum peak at the tuning frequency from other peaks because of the noise. In these figures, the abscissa is the time and the ordinate is the measured frequency and strain. These figures suggest that the tuning frequency decreases with increase of the applied tensile strain. This characteristic agrees with the static tensile test shown in figure 12. From figure 13(b), the tuning frequency changes according to the strain change wirelessly at the stroke frequency of 10 Hz.

Figure 14 shows results for the relationship between the tuning frequency and the applied strain at stroke frequencies of 0.5, 1, 5, and 10 Hz. The tuning frequency and the applied strain mutually correspond. These results indicate that the proposed method is applicable for wireless strain measurement of commercially available tyres.

5. Conclusions

The present study proposes a novel passive wireless method for measuring tyre strain. The method requires no additional sensors. Instead, it employs the tyre itself as a sensor.

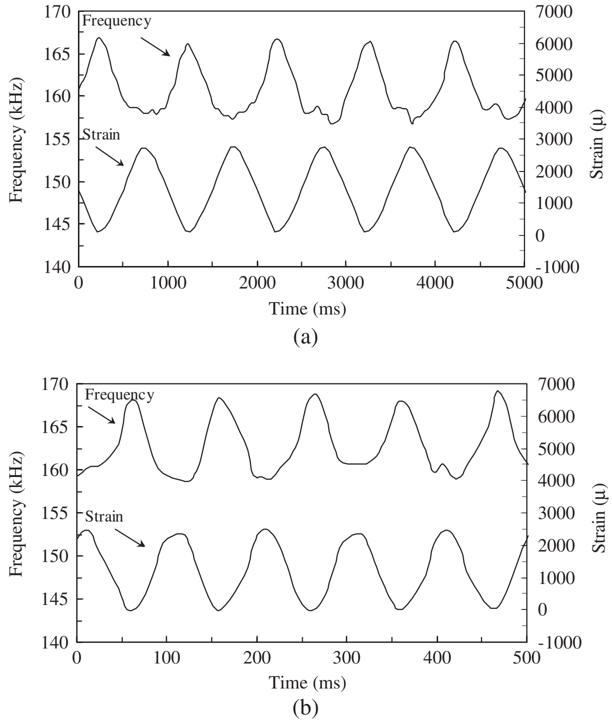

Figure 13. Measured tuning frequency change of the passive wireless sensor and strain change. (a) Stroke frequency: 1 Hz. (b) Stroke frequency: 10 Hz.

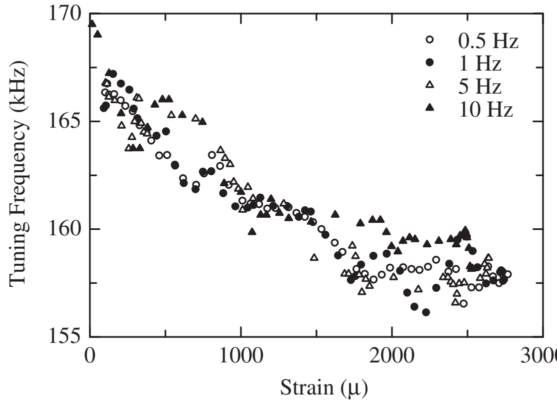

Figure 14. Measured relationships between tuning frequency and strain.

Therefore, it does not disturb the tyre stress and deformation field. Moreover, sensor debonding is impossible. Steel wires of the tyre are adopted as electrodes to charge high-frequency alternating current. Tyre deformation changes the capacitance of the tyre. The tyre is connected to a simple tuning circuit as a condenser. Thereby, the capacitance change of the tyre is converted to a tuning frequency change of the LC resonant circuit. The method is demonstrated using a rectangular specimen cut from a commercially available radial tyre.

(1) The capacitance of the tyre increases with increase of the tensile loading. The increase of the capacitance is caused by the decrease of the spacing of steel wires in the tyre during loading.

(2) The tyre specimen is connected to the sensor circuit as a condenser. The tuning frequency of the sensor circuit is measured wirelessly without any power supply to the sensor circuit.
(3) The proposed passive wireless strain measurement method is demonstrated experimentally with static tension tests and cyclic loading tests. The tuning frequency of the sensor circuit decreases with increase of the tensile loading even at the high stroke frequency of 10 Hz.

Acknowledgment

Financial support from Bridgestone Corp. in Japan is acknowledged.

References

[1] Mnif K 2001 A smart tire pressure monitoring system *Sensors* **18** 40–6
[2] Cullen J D, Arvanitis N, Lucas J and Al-Shamma'a A I 2002 In-field trials of a tyre pressure monitoring system based on segmented capacitance rings *Measurement* **32–3** 181–92
[3] Yamagiwa T, Orita M and Harada T 2003 Development of a tire pressure monitoring system for motorcycles *JSAE Rev.* **24-4** 495–6
[4] Umeno T, Asano K, Ohashi H, Yonetani M, Naitou T and Taguchi T 2001 Observer based estimation of parameter variations and its application to tire pressure diagnosis *Control Eng. Pract.* **9** 639–45
[5] Persson N, Ahlqvist S, Forssell U and Gustafsson F 1999 Low tyre pressure warning system using sensor fusion *SAE Conf. Proc.* pp 77–9
[6] Pohl A, Steindl R and Reindl L 1999 The 'intelligent tire' utilizing passive saw sensors—measurement of tire friction *IEEE Trans. Instrum. Meas.* **48-6** 1041–6
[7] Gavine A 2001 Common sense? The latest in vehicle safety comes courtesy of continental with its potentially life-saving tread deformation sensor *Tire Technol. Int.* (September) 32–3
[8] Parwardhan S, Tan H S and Tomizuka M 1977 Experimental results of a tire burst controller for AHS *Control Eng. Pract.* **5–11** 1615–22
[9] Palmer M E, Boyd C C, McManus J and Meller S 2002 Wireless smart-tire for road friction measurement and self state determination *43rd AIAA/ASME/ASCE/AHS Structure, Structural Dynamics, and Materials Conf.* AIAA-2002-1548
[10] Matsuzaki R and Todoroki A 2005 Wireless strain monitoring of tires using electrical capacitance changes with an oscillating circuit *Sensors Actuators* A **119** 323–31
[11] Matsuzaki R, Todoroki A, Kobayashi H and Shimamura Y 2005 Passive wireless strain monitoring of a tire using capacitance and electromagnetic induction change *Adv. Compos. Mater.* at press
[12] Brandt M, Bachmann V, Vogt A, Fach M, Mayer K, Breuer B and Hartnagel H L 1998 Highly sensitive AlGaAs/GaAs position sensors for measurement of tyre tread deformation *Electron. Lett.* **34–8** 760–2
[13] Yilmazoglu O, Brandt M, Sigmund J, Genc E and Hartnagel H L 2001 Integrated InAs/GaSb 3D magnetic field sensors for 'the intelligent tire' *Sensors Actuators* A **94** 59–63
[14] Varadan V V, Varadan V K, Bao X, Ramanathan S and Piscotty D 1997 Wireless passive IDT strain microsensor *Smart Mater. Struct.* **6** 745–51
[15] Hautamaki C, Zurn S, Mantell S C and Polla D L 1999 Experimental evaluation of MEMS strain sensors embedded in composites *J. Microelectromech. Syst.* **8** 272–9
[16] Sherlock B G 1999 Windowed discrete Fourier transform for shifting data *Signal Process.* **74** 169–77
[17] Rosvall S J M, Honeychurch M J, Elton D M and Bond A M 2001 A practical approach to applying short time Fourier transform methods in voltammetric investigations *J. Electroanal. Chem.* **515** 8–16
[18] Amemiya K, Moriwaki S and Mio N 2003 Use of the maximum-entropy method for measuring the resonance of a mechanical oscillator *Phys. Lett.* A **315** 184–8